International Journal of Nanomedicine

Dovepress
open access to scientific and medical research

Open Access Full Text Article

ORIGINAL RESEARCH

MSC-Derived Exosomes Mitigate Myocardial Ischemia/Reperfusion Injury by Reducing Neutrophil Infiltration and the Formation of Neutrophil Extracellular Traps

Yuting Feng, Xue Bao, Jinxuan Zhao, Lina Kang, Xuan Sun, Biao Xu

Department of Cardiology, Nanjing Drum Tower Hospital, State Key Laboratory of Pharmaceutical Biotechnology, Medical School of Nanjing University, Nanjing, People's Republic of China

Correspondence: Xuan Sun; Biao Xu, Department of Cardiology, Nanjing Drum Tower Hospital, State Key Laboratory of Pharmaceutical Biotechnology, Medical School of Nanjing University, No. 321 Zhongshan Road, Nanjing, 210008, People's Republic of China, Email sunxuan891119@163.com; xubiao62@nju.edu.cn

Introduction: Acute inflammatory storm is a major cause of myocardial ischemia/reperfusion (I/R) injury, with no effective treatment currently available. The excessive aggregation of neutrophils is correlated with an unfavorable prognosis in acute myocardial infarction (AMI) patients. Exosomes derived from mesenchymal stromal cells (MSC-Exo) have certain immunomodulatory potential and might be a therapeutic application. Therefore, we investigated the protective role of MSC-Exo in modulating neutrophil infiltration and formation of neutrophil extracellular traps (NETs) following myocardial I/R injury.

Methods: Exosomes were isolated from the supernatant of MSCs using a gradient centrifugation method. We used flow cytometry, histochemistry, and immunofluorescence to detect the changes of neutrophils post-intravenous MSC-Exo injection. Additionally, cardiac magnetic resonance (CMR) and thioflavin S experiments were applied to detect microvascular obstruction (MVO). The NLR family pyrin domain containing 3 (NLRP3) inflammasome was examined for mechanism exploration. Primary neutrophils were extracted for in vitro experiment. Antibody of Ly6G was given to depleting the neutrophils in mice for verification the effect of MSC-Exo. Finally, we analyzed the MiRNA sequence of MSC-Exo and verified it in vitro.

Results: MSC-Exo administration reduced neutrophil infiltration and NETs formation after myocardial I/R. MSC-Exo treatment also could attenuate the activation of NLRP3 inflammasome both in vivo and in vitro. At the same time, the infarction size and MVO following I/R injury were reduced by MSC-Exo. Moreover, systemic depletion of neutrophils partly negated the therapeutic effects of MSC-Exo. Up-regulation of miR-199 in neutrophils has been shown to decrease the expression of NETs formation after stimulation.

Discussion: Our results demonstrated that MSC-Exo mitigated myocardial I/R injury in mice by modulating neutrophil infiltration and NETs formation. This study provides novel insights into the potential therapeutic application of MSC-Exo for myocardial ischemia/reperfusion injury.

Keywords: myocardial ischemia/reperfusion injury, mesenchymal stromal cells, exosomes, neutrophil extracellular traps, mir-199

Introduction

Acute myocardial infarction (AMI) has been a major cause of death and heart failure (HF) worldwide in current. Percutaneous coronary intervention (PCI) to recanalize the artery in the early stage of AMI salvages the injured myocardium and improves survival. However, the rapid restoration of blood flow triggers ischemia/reperfusion (I/R) injury,[1] which reduces the curative effect of PCI.

The inflammatory response is one of the important pathological mechanisms of myocardial I/R injury.[2] Neutrophils play a pivotal role in mediating inflammation as the first immune cells recruited from the bloodstream into injured tissues.[3] The number and proportion of neutrophils in the peripheral blood and myocardium tissue increase rapidly in the

Received: 19 September 2023
Accepted: 14 February 2024
Published: 5 March 2024

Graphical Abstract

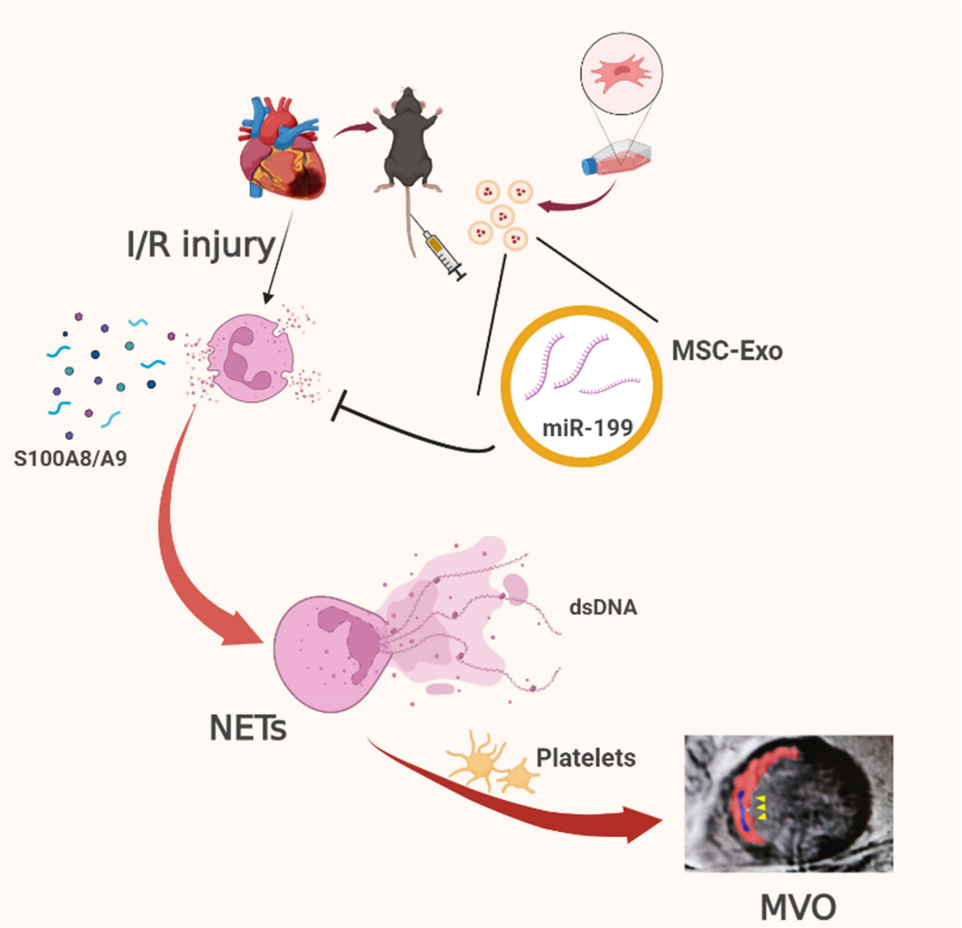

acute phase of I/R injury and the infiltration of neutrophils in the myocardium reaches the peak within 24 hours after reperfusion. Neutrophils remove necrotic debris at the injured site and recruit the mononuclear macrophage system for further repair.[4] But the excessive aggregation and activation of neutrophils result in the release of a plethora of damage-associated molecular patterns (DAMPs) and inflammatory cytokines, which subsequently contribute to myocardial necrosis, aggravated ventricular remodeling, and reduced cardiac function.[5]

Activated neutrophils can release neutrophil extracellular traps (NETs), manifesting as weblike DNA structures decorated with histones and antimicrobial proteins.[6] The released NETs bind to platelets and red blood cells and then finally form plugs. These plugs are dispersed by blood flow into microvessels, forming embolisms that impede tissue perfusion despite the restoration of large coronary arteries.[7] This phenomenon, known as microvascular obstruction (MVO), is a major contributor to I/R injury and infarct size, and an increased risk of developing heart failure after AMI.[8] Besides, NETs promote the formation of reactive oxygen species[9] and the secretion of inflammatory factors and chemokines to aggravate the inflammatory response.[10] Neutrophils have also been proven as the primary source of the proinflammatory alarmins, S100A8 and S100A9, after AMI.[11] The release of S100A8 and S100A9 in the myocardium stimulates additional leukocyte recruitment and increases the secretion of pro-inflammatory cytokines.[12] High plasma levels of S100A8 and S100A9 after PCI are associated with poor left ventricular ejection fraction (LVEF) and an increased incidence of HF[13] in AMI patients. These pathological processes above finally result in a vicious circle of

myocardium injury. Neutrophil influx and NETs are associated with poor outcomes after cardiac ischemia. However, there are currently not any clinically approved interventions able to modulate neutrophils after I/R injury.

Mesenchymal stromal cells (MSCs) have been demonstrated to have immunomodulatory properties[14] and the therapeutic applications of MSCs are being explored in cardiovascular diseases.[15] However, the risk of thrombosis formation and immunoreactivity have suggested that caution is still warranted in the clinical use of MSCs.[16] The exosomes secreted by MSCs (MSC-Exo) have been known to mediate cell-to-cell communication, which has well-established anti-inflammatory effects.[17] We have reported that MSC-Exo plays a protective effect on ischemic myocardium by polarizing inflammatory macrophage towards an anti-inflammatory macrophage population.[18] In consideration that neutrophils infiltration into the myocardium peaks within 24 hours after reperfusion and they are prime drivers of the pro-inflammatory phase, it remains unknown whether MSC-Exo could inhibit neutrophils from mobilization, recruitment or MVO formation thus limiting inflammation.

In this study, we assessed whether MSC-Exo therapy in the early stage could suppress neutrophil infiltration and NETs formation to preserve cardiac function. Our research has shown the promising effect of MSC-Exo in myocardium I/R injury.

Materials and Methods

Study Patients Analysis

Peripheral blood from AMI patients was collected at the Department of Cardiology in Nanjing Drum Tower Hospital. In total, 71 patients with ST elevation myocardial infarction (STEMI) were enrolled, and they received PCI within 24 hours of showing symptoms. Demographic characteristics (age, gender, heart rate, body mass index, Killip class, blood pressure, and symptom onset to balloon time) and previous history (pre-infarction angina and smoking) were recorded in medical files while hospitalized. Exclusion criteria included contraindications to cardiac magnetic resonance (CMR) and those having symptoms or a history of infection in the last month, like autoimmune diseases, AIDS, cancer and so on. Ethical approval for the human study was obtained from the Institutional Ethics Committee of Nanjing Drum Tower Hospital (approval number, 2019–190-01), and all human subjects provided informed consent. This study was conducted in accordance with the Declaration of Helsinki. Meanwhile, the human demographic information was shown in Table 1.

Two-dimensional transthoracic echocardiography was performed within 3 days after primary PCI. LVEF was evaluated using Simpson's biplane technique. Left atrial diameter (LAD) and left ventricular end-diastolic diameter (LVEDd) were obtained by echocardiography.

Table 1 Clinical Characteristics of Patients and Healthy People

Variable	Control, N = 35	MVO, N = 35	NO MVO, N = 36	p-value
Age, year	55.08±9.554[a]	61.94±12.751[b]	57.97±11.106[a]	0.039
BMI	25.4448±2.839070	25.2973±4.703455	25.2111±8.333122	0.986
Gender, male (%)	34 (97.1%)[b]	28 (80%)[a,b]	35 (97.2%)[a]	0.012
Heart rate, bpm	81 (73, 86)	81 (70, 98)	83 (71, 98)	0.140
Smoke, n (%)	9 (25.7%)[b]	24 (68.6%)[a]	27 (75%)[a]	<0.001
Drink, n (%)	9 (25.7%)	8 (22.9%)	6 (16.7%)	0.639
Diabetes mellitus, n(%)	2 (5.7%)[b]	11 (31.4%)[a]	12 (33.3%)[a]	0.010
Hypertension, n(%)	10 (28.6%)[b]	22 (62.9%)[a]	20 (55.6%)[a]	0.010
Stroke, n(%)	1 (2.9%)	2 (5.7%)	2 (5.6%)	0.817
eGFR, mL/min/1.73m2	102.775±16.0433	104.988±26.0857	116.439±22.2011	0.400
LDL, mmol/L	2.9406±0.769545	2.7732±1.044581	2.7042±0.856724	0.267
Killip class	/	1.08±0.439	1.11±0.323	0.460

Notes: Data are reported as the mean±standard deviation or N (%) where appropriate. P values have been obtained from one-way ANOVA with Bonferroni correction, Kruskal–Wallis test, or Fisher test. For the variables in the same row with the same letter "a" or "b", the difference is not statistically significant. If two variables have different letters, they are significantly different.

Abbreviations: MVO, Patients with microvascular obstruction group; NO MVO, Patients without microvascular obstruction group; BMI, Body mass index; eGFR, Estimated glomerular filtration rate; LDL, Low-density lipoprotein.

Laboratory Assays

The blood sample of subjects was collected 6 hours after PCI. Blood routine examination and levels of cardiac high-sensitive troponin T (cTNT), creatine kinase MB (CK-MB), and brain natriuretic peptide (BNP) were measured in the hospital biochemistry laboratory. S100A8/A9 protein levels were measured by commercial enzyme-linked immunosorbent assay kits according to the manufacturer's instructions (R&D, DS8900). For the quantification of double-stranded DNA (dsDNA), a Quant-iTPicoGreen dsDNA Assay (Invitrogen, P11496) with a sensitivity of 0.25 pg/mL was used.

CMR Imaging

CMR was performed 7 days after primary PCI. CMR protocol and standardized postprocessing were conducted on 3.0 T CMR for left ventricular function and standard infarction characteristics (infarct size, MVO, and strain) as previously described.[19] Briefly, cine images were obtained 5 minutes after injection of extracellular gadolinium-based contrast agent for left ventricular function. Endocardial and epicardial borders were manually traced to calculate left ventricular end-diastolic volume (LVEDV). MVO was defined as the absence of contrast wash-in inside the delayed gadolinium-enhanced area. The global radial, circumferential, and longitudinal strains were detected as previously described.

Animal Experimental Protocol

All procedures with animals were approved by the Institutional Ethics Committee of Nanjing Drum Tower Hospital and performed in accordance with the guidelines set forth in the Guide for the Care and Use of Laboratory Animals published by the National Institutes of Health (Eighth Edition).

The myocardial ischemia/reperfusion (I/R) injury model was established on male C57BL/6J mice at 8 weeks of age, purchased from Gem Pharma tech Co. Ltd (Jiangsu, China). After mice were anesthetized by intraperitoneal administration of ketamine (100 mg/kg) and xylazine (10 mg/kg) and ventilated by a rodent ventilator with room air. A left lateral intercostal thoracotomy was performed to expose the heart. The left anterior descending coronary artery (LAD) was ligated with a 7–0 silk suture for 45 minutes of ischemia and then released to form reperfusion. Instantly after reperfusion, a dose of 100 μL PBS containing exosomes at 3ug/g of body weight was administered via a caudal vein to each mouse in the MSC-Exo group as previous reported.[20–22] In the sham group, the left lateral intercostal thoracotomy was performed without ligation of the artery. In the control group, the mice were not treated with any operations. Each group consisted of at least six mice.

Neutrophil Depletion

To determine the role of neutrophils after MSC-Exo injection in AMI, mice were intraperitoneally treated with anti-Ly6G antibody (BioLegend, 127649) at 100 μg per mouse as previous study described.[23] After 24 hours, the mice were used for I/R model establishment.

Echocardiography Assessment

At the designated time points (24 hours, 3 days, 4 weeks) after I/R models were established, the mice were anesthetized with isoflurane gas and then assessed with VEVO2100 Biomicroscope (VisualSonics). Left ventricular ejection fraction (LVEF%) and LV fractional shortening (FS%) were calculated within at least three consecutive cardiac cycles in both of long axis view and short axis.

Myocardial Infarct Size Measurements

The heart was stained by Evan's blue dye and 2,3,5-triphenyl-2H-tetrazolium chloride (TTC) to indicate the myocardial infarct size. Three days after I/R injury, thoracotomy was operated again and the LAD was ligated at the same site as before. 0.2 mL 1% Evan's blue dye was injected into the aortic root and then the heart was immediately excised. After frozen at −80°C, the heart was cut into 1.2-mm thick slices perpendicularly from apex. The slices were soaked in 1.5% TTC in the dark at room temperature for 15 minutes and then were digitally imaged and analyzed using the computer-based image analyzer Image J software (version 1.53). The blue area stained by Evan's blue dye represented the no-risk

area, while the unstained indicated the area at risk (AAR). AAR was separated into the red section which was stained by TTC and the pale section representing the infarct size (IS). The percentage of AAR and IS could be calculated as follow, AAR%= (AAR area/total area of myocardium) × 100%; IS%= (infarct area/AAR) × 100%.

Fluorescence-Activated Cell Sorting (FACS) Analysis

Mice were euthanized to collect peripheral blood samples and retrogradely perfused in the heart with cold normal saline to get ventricle samples. Blood samples were loaded in anticoagulant tubes and the ventricles were minced with Medimachine (BD Biosciences Pharmingen) in PBS with 1% FBS to prepare a single-cell suspension. Neutrophils were stained with antibodies against CD45-APC (eBioscience, 17–0451-82) Ly6g-FITC (eBioscience, 12–5931-82) and the platelets were stained with CD41-PE (Biolegend, 127649) for 1 hour at 4°C with rotation, avoiding from light. After incubation, the blood samples were treated with lysis buffer to remove the red blood cells. Samples were detected by a FACS Calibur flow cytometer (BD FACS Calibur) and analyzed by FlowJo 10.1 software (Tree Star).

Histological and Immunohistochemistry Analysis

The heart was integrally excised at the scheduled time after I/R injury and fixed with 4% formalin. After dehydration and embedding in paraffin, the myocardium tissue was cut into 5μm sections perpendicularly from apex for subsequent stains. To analyze the morphology and inflammatory infiltration, the sections were stained were hematoxylin and eosin and observed in 10 randomly selected visual fields. The sections were also stained by Masson trichrome for collagen (blue stained) volume fraction calculating to analyze cardiac fibrosis.

To determine the distribution of neutrophils or neutrophil extracellular traps (NETs) in the myocardium, the deparaffinized tissue sections were incubated with anti-Ly6g antibody (Abcam, ab121272) or anti-Histone H3 (citrulline R2 + R8 + R17) antibody (Abcam, ab5103) overnight at 4°C. After being washed with PBS, the tissues were incubated with a biotin-conjugated secondary antibody and then treated with Avidin-Biotin complex reagent. Hydrogen peroxide and 3–3′ diaminobenzidine tetrachloride (DAB) were used to develop the stain.

For immunofluorescence staining, the heart was quick-frozen in liquid nitrogen and cut into 5μm sections. Fixed with 4%PFA and blocked with 5% bovine serum in PBS, the cryosections were permeabilized with 0.1% Triton-X 100. After incubation with primary antibodies overnight at 4°C. To determine Nlrp3 and NETs distribution, we stained the slides with Alex488-conjugated Nlrp3 antibody (Abcam, ab270449) or co-stained with Alex488-conjugated H3Cit and Alex647-conjugated MPO antibody (R&D systems, BAF3667). Then nuclei were counterstained with DAPI. Digital images were photographed by a conventional fluorescence microscope (Leica Thunder, Germany). Randomly selected 10 microscopic views which covered a 1mm² area were analyzed.

TUNEL Staining

To investigate the cell apoptosis in the I/R injury myocardium, the heart was quick-frozen in liquid nitrogen and cut into 5μm sections. After fixing with 4% PFA, the slides were treated with TUNEL staining according to the manufacturer's instructions (Roche, 12156792910). To determine cardiomyocyte size, we used an Alexa Fluor 488–conjugated α-actinin and DAPI. Randomly selected 10 microscopic views which covered a 1 mm² area were analyzed.

Dextran Staining

To display the vascular permeability, the mice were injected by tail vein with 500μL 10% dextran-FITC in PBS. After 5 minutes the mice were killed and the hearts were excised. Washed in the cold PBS to remove blood, the hearts were quick-frozen and cut into cryosections as previously mentioned. Nuclei were counterstained with DAPI. Randomly selected 10 microscopic views which covered a 1 mm² area were analyzed.

Thioflavin S Staining

To evaluate the "no-reflow" area, 4% fluorescent dye thioflavin S (1mL/kg, Sigma-Aldrich) saline solution was injected into the heart through the carotid artery instantly after the heart was excised. Then the hearts were frozen in the −80°C fridge and sectioned at 1.2-mm intervals. Normal areas fluoresced under ultraviolet light, whereas the microvascular

obstruction area remained dark. Photos were digitally imaged and analyzed using the computer-based image analyzer Image J software.

Cardiac Magnetic Resonance Imaging on Mice

CMR measurements were performed with a 9.4T-Tesla MRI (BioSpec 94/20 USR). Animal anesthesia was induced by inhalation of 4% isoflurane and maintained at 1–2% isoflurane mixed with air during the examination. A respiratory balloon was placed on the abdomen under the sternum to monitor respiration, and 3 ECG leads were inserted subcutaneously on the left forelimb, right forelimb, and right hind limb for ECG tracing. For systolic function measurements, a series of prospective ECG- and respiratory-triggered short-axis CINE movies were acquired covering the heart from apex to base with a FLASH sequence.

Cell Isolation and Culture

Mouse bone marrow-derived MSCs were generally isolated from the tibia and femoral marrow compartments and were identified by flow cytometry as described previously.[18] The cells cultured in MSC culture medium (Science Cell, 7501) with 1% mesenchymal stem cell growth supplement (Science Cell,7552), 5% fetal bovine serum (Science Cell,0025) and 1% Penicillin/Streptomycin (Science Cell,0503). The cell incubator was maintained at 37°C with 5% CO_2 and 95% humidity. Every 2–3 days the culture medium was changed and Trypsin-EDTA (0.25%) (Gibco, 25200056) was used for passaging.

Neutrophils were isolated from bone marrow of 4-week-old C57BL/6J mice. The femur and tibia were resected intactly and cut the two ends of the bone in a clean bench to flush the bone marrow out. After treatment with red cell lysis buffer, the neutrophils were isolated using Mouse neutrophil isolation kit (Miltenyi Biotec, 130–097-658) according to the manual. The isolated neutrophils were cultured in RPMI1640 medium supplemented with 10%FBS for future use.

Exosome Isolation

Replace the culture medium with one containing 5% exosome-depleted fetal bovine serum (System Biosciences, EXO-FBS-250A-1) when the MSCs reached 70–80% confluency. 48 hours later, the supernatants were collected and centrifuged at 3000g for 30 minutes and 10,000g for 1 hour at 4°C in order to remove impurities such as cell debris. Finally, the supernatants were centrifuged at 50,000g for 2 hours at 4°C to precipitate exosomes. The exosomes were resuspended in pre-cold sterile PBS and stored at −80°C for use.

Labelling of Exosomes

To observe the internalization of MSC-Exo into neutrophils, exosomes were labeled with DiD dye (Beyotime, C1995S) according to the manufacturer's instructions and washed with PBS followed by centrifugation at 50,000g for 1 h at 4 °C. Then, the DiD-labeled MSC-Exo were co-cultured with primary neutrophils at a final concentration of 20 μg/mL. After 6 hours, the cells were washed with PBS and stained with DAPI. Finally, the cells were examined and photographed with a conventional fluorescence microscope (Leica Thunder, Germany). ImageJ software was used to measure uptake as whole image fluorescence intensity for neutrophils.

Live Cell Imaging

The live cell imaging was performed with imaging media consisting of RPMI 1640 lacking Phenol red (Fisher Scientific, 11835030) with 25nM HEPES (ThermoFisher, 15630080) and 1% Penicillin/Streptomycin (ThermoFisher, 10378016). Cells were incubated with SiR-DNA (Cytoskeleton, CY-SC007) for 30 min at 0.5 μM concentration before being washed and then resuspended in imaging media. Digital images were photographed by a conventional fluorescence microscope (Leica Thunder, Germany) in rapid succession acquired every 5 minutes for 2 hours.

Cytokine Analysis in Peripheral Blood and Cell Culture Supernatants

Whole blood samples of mice were collected and centrifuged at 300g for 20 minutes to obtain plasma. The cell culture supernatants were also harvested 24 hours after being stimulated with PMA. The protein levels of IL-1β were detected

using a mouse IL-1β High Sensitivity ELISA kit (Multi Science, EK201BHS) and S100A8/A9 dimer were detected using Mouse S100A8/S100A9 Heterodimer DuoSet ELISA (R&D Systems, DY8596-05) following the instructions.

RNA Isolation and Quantitative Real-time PCR

Total RNA was extracted from heart tissues and cells using TRIzol reagent (Invitrogen, 15596018CN) according to the instructions. A NanoDrop Spectrophotometer (ThermoFisher Scientific) was used to detect the concentration and purity of RNA. To detect the gene expression, RNA was reverse transcribed into DNA using a HiScript II 1st Strand cDNA Synthesis Kit (Vazyme R223-01), and then Quantitative real-time PCR was performed using the ChamQ SYBR qPCR Master Mix (Vazyme Q711-02/03). To assess the expression of miRNA, RNA was treated with miRNA 1st Strand cDNA Synthesis Kit (Vazyme MR101-02). The cDNA was used for Quantitative real-time PCR with miRNA Universal SYBR qPCR Master Mix (Vazyme MQ101-02). The expression of 18S was used as a reference gene to normalize the RNA content of each gene. The relative gene expression level was calculated using the 2 - ΔΔCt method. The sequences of the primers are shown in Table S1.

Western Blotting

The Nlrp3 signal pathway, PAD4, H3Cit and MPO expression in the myocardium tissues with/without I/R injury and neutrophils stimulated by PMA were detected. The left ventricles and neutrophils were lysed in lysis buffer with 1uM for at least 30 minutes on ice and then centrifuged at 12,000rpm for 10 minutes to remove the sediment. Total protein concentration was assessed by BCA assay (ThermoFisher Scientific, 23225) according to the instruction. Samples of 10–30μg were loaded on 4–12% Bis-Tris SDS-page and transferred onto PVDF membranes (Millipore). Membranes were blocked with 5% skim milk in TBS-Tween (0.1%) and incubated against the desired antibodies overnight at 4 °C. GAPDH was used as loading control. Detection was carried out using peroxidase-coupled corresponding second antibodies at 1:10,000 for 1 hour at room temperature. Protein bands were visualized using enhanced chemiluminescence (ThermoFisher Scientific, 32106).

Transfection of miRNA Mimics and Inhibitors

3×10^6 Mouse neutrophils were transfected with the miRNA mimics (50nM, Ribobio) or miRNA inhibitors (100nM, Ribobio) or negative controls using Lipofectamine 2000 (Invitrogen) according to the manufacturer's instructions. After 6 hours, the culture medium was replaced with RPMI1640 medium and the cells were stimulated with PMA 24 hours after transfection. Scrambled pre-microRNA was used as a negative control. The effect of transfection was examined by qRT-PCR. The cells were harvested 24 hours after stimulation.

MSCs were transfected with 100 nM of miR-199a-5p or miR-199a-3p inhibitor (Ribobio) following the manufacturer's instructions. After 6h transfection, culture medium was changed with that containing exosome-depleted FBS for exosome isolation. The effect of transfection was examined by qRT-PCR.

RNA-Seq

Total RNA isolated from neutrophils was degraded and contamination was monitored on 1% agarose gels, and its purity was checked using the NanoPhotometer spectrophotometer (IMPLEN, CA, USA). A library was prepared according to the method and process of NEBNext UltraTM RNA Library Prep Kit for Illumina (NEB, USA). Deep sequencing of the RNA profiles was performed with an Illumina Novaseq platform and 150 bp paired-end reads were generated. The data output was received in Excel spreadsheets, and GO enrichment analysis were demonstrated in Bubble map.

Statistical Analysis

The data from a minimum of three independent experiments were presented as mean ± SD. Differences between groups at a single time point were determined using either a two-tailed, unpaired Student's *t*-test or one-way analysis of variance (ANOVA) followed by Tukey's multiple comparisons test. Differences between groups at multiple time points were determined using two-way ANOVA followed by Bonferroni's multiple comparisons test. All statistical analyses were

conducted using Prism 6 software (GraphPad), and only differences with a P-value less than 0.05 were considered statistically significant.

Results

The Counts of Neutrophils Were Negatively Related to the Outcomes in AMI Patients

To investigate the relationship between neutrophils and MVO in AMI patients, 71 patients with an ongoing AMI and 35 healthy people were recruited for the trial. The baseline clinical characteristics of the groups were presented in Table 1.

According to the data, the echocardiography results during follow-up were negatively correlated with the percentage and counts of neutrophils (Figure 1A and B). The plasma analysis showed that a higher level of S100A8/A9 was related to lower ejection fraction (EF%) (Figure 1C). Besides, plasma double-stranded DNA (dsDNA) as the surrogate marker of NETs,[8] which the concentration of was also correlated negatively with cardiac function (Figure 1D). The magnetic resonance imaging analysis revealed a direct correlation between the extent of myocardial damage and the concentration of neutrophils in the bloodstream (Figure 1E).

MVO has been demonstrated as a strong predictor of cardiac inflammation and cardiac insufficiency and our data also supported it (Figure 1F and G). There were significant differences in neutrophil percentage and counts between patients with or without MVO formation (Figure 1H and I). S100A8/A9 concentration in plasma was markedly increased in patients after AMI, especially in those with MVO (Figure 1J). Furthermore, the AMI patients in the MVO group showed a higher plasma dsDNA concentration level than those patients without MVO (Figure 1K). These data revealed that the elevated level of neutrophils after AMI might be relevant to the formation of MVO and finally have an influence on cardiac function.

Characterization of MSC-Exo

Exosomes were isolated from the supernatants of MSCs using serial differential centrifugation plus ultracentrifugation. The exosomes were characterized by nanoparticle tracking analysis (NTA) and transmission electron microscopy (Figure S1A and B). Western blot analysis confirmed the expression of HSP70, CD63, and TSG101 of the particles (Figure S1C), which were well-established molecular markers of exosomes.

MSC-Exo Reduced Neutrophil Infiltration and NETs Release Following Myocardial I/R Injury

In vivo, flow cytometry analysis showed that the proportion of CD11b+Ly6g+ neutrophils was significantly increased in the heart tissues and peripheral blood during 6 to 72 hours after I/R injury (Figure 2A–C and Figure S2). The proportion of neutrophils in the MSC-Exo-treated group was remarkably reduced in peripheral blood 12 hours after I/R injury, compared with the PBS-treated group. In damaged myocardium tissue, the neutrophils decreased by MSC-Exo 24 hours after reperfusion. It is well recognized that activated platelets are a major role to induce the NETs formation after binding to the neutrophils.[24] The amount of neutrophil-platelet complex (Ly6g+CD41+ cell) was significantly reduced by MSC-Exo treatment in heart tissues (Figure 2D). Hematoxylin and eosin (HE) staining showed that there was more inflammatory cells infiltration in the myocardium of mice treated with PBS than with MSC-Exo (Figure 2E). Ly6G immunohistochemical (IHC) analysis showed more neutrophils infiltration in the PBS group than that in the MSC-Exo group (Figure 2F). The myocardial tissue analysis revealed the decreased expression of CXCL1 and CXCL2 (Figure 2H–J), indicating the reduced neutrophil accumulation by MSC-Exo administration. The immunofluorescence staining showed that NETs formation was decreased in the MSC-Exo treatment group compared to the PBS group (Figure 2G). H3Cit IHC analysis also revealed that MSC-Exo reduced the NETs released (Figure 2F). PAD4 has been demonstrated as a regulator of NETs release.[19] Western blot analysis of H3Cit, MPO, and PAD4 proved the inhibition of NETs in the myocardium by MSC-Exo treatment (Figure 2J and K). Furthermore, the concentration of dsDNA in plasma was also decreased in the MSC-Exo-treated group (Figure 2L). These results above indicated that the MSC-Exo could inhibit neutrophil infiltration and NETs release in the acute phase of myocardial I/R injury.

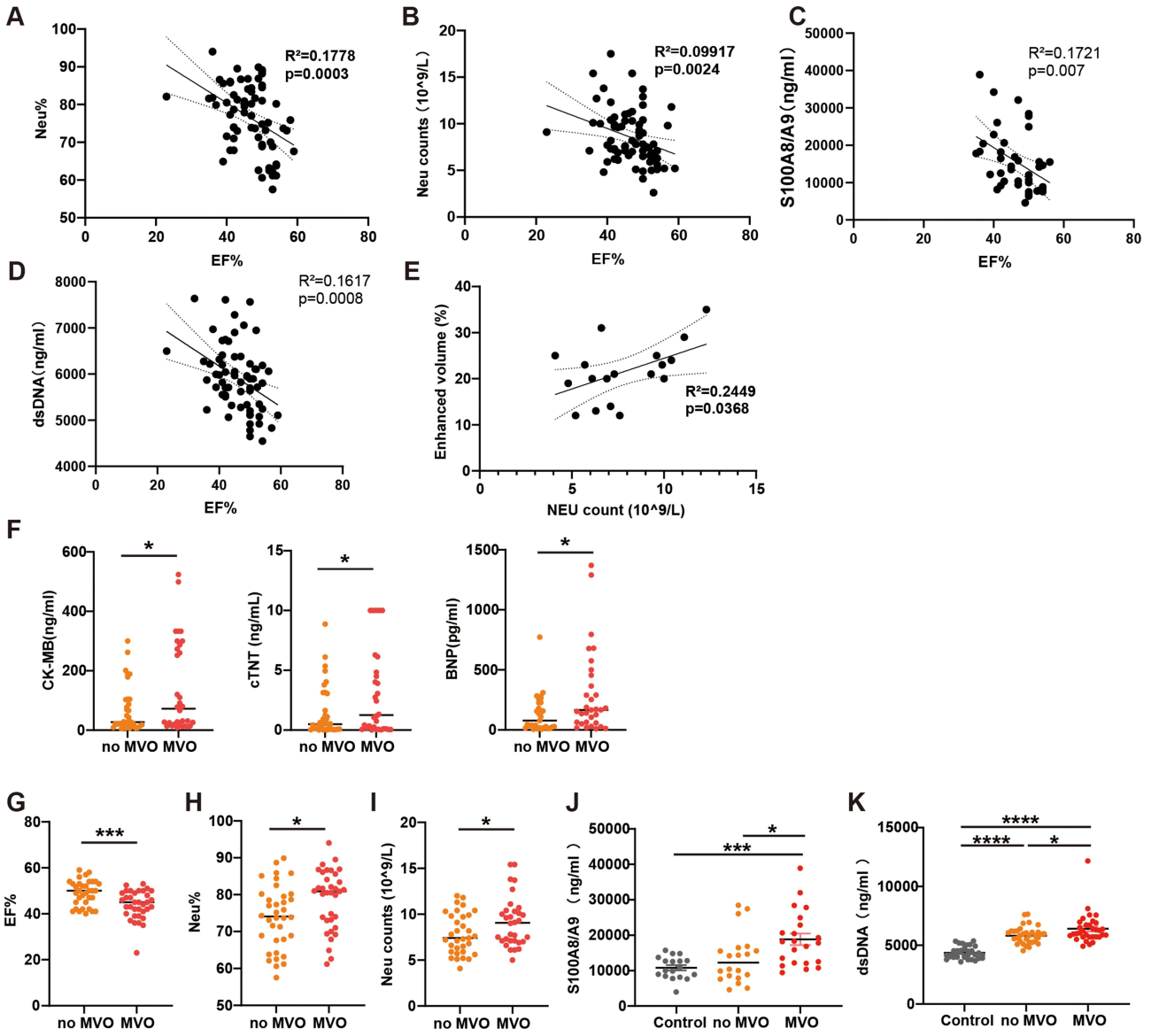

Figure 1 Increased levels of neutrophils are associated with MVO and LV function in patients with STEMI. (**A** and **B**) Correlation between EF% measured by echocardiography and the proportion (**A**), counts (**B**) of neutrophils in blood routine of AMI patients 6 hours post-PCI (n=71). (**C**) Correlation between plasma S100A8/a9 concentration and EF% in AMI patients (n=43). (**D**) Correlation between plasma dsDNA concentration and EF% in AMI patients (n=67). (**E**) Correlation between the percentage of enhanced volume measured by cardiac magnetic resonance imaging and counts of neutrophils in blood routine of AMI patients (n=18). (**F**) Plasma creatine CK-MB, cTNT, and BNP concentrations in AMI patients with MVO (n=32) and without MVO (n=31). (**G–I**) EF% (**G**), the proportion (**H**), and counts (**I**) of neutrophils in AMI patients with MVO (n=32) and without MVO (n=33). (**J**) Concentration of plasma S100A8/A9 in control group (n=18), AMI patients with MVO (n=22) and without MVO (n=20). (**K**) Concentration of plasma dsDNA in control group (n=35), AMI patients with MVO (n=33) and without MVO (n=34). In panels A-E, p value as shown (Pearson's correlation). In panels F-I, *p < 0.05, ***P<0.001 (unpaired two-tailed Student's *t*-test). In panels (**J** and **K**), *P<0.05, ***P<0.001, ****P<0.0001 (one-way ANOVA with Bonferroni correction).

To investigate whether the MSC-Exo could affect neutrophils directly, we added MSC-Exo to the cultured primary neutrophils. The DiD-labelled exosomes were ingested by neutrophils within 6 hours (Figure 3A). RNA sequencing of neutrophils was performed in vitro to illustrate the effects of MSC-Exo on neutrophils. PMA was used as an inflammatory stimulus for neutrophils. After 12 hours, RNA was extracted for sequencing. As shown in the biological process analysis, MSC-Exo had effects on the extracellular matrix and structure organization (Figure 3B). According to previous reports, NETs formation results in the release of cellular contents and is associated with the remodeling of the extracellular matrix.[6] These data revealed that MSC-Exo may have an influence on the NETs formation.

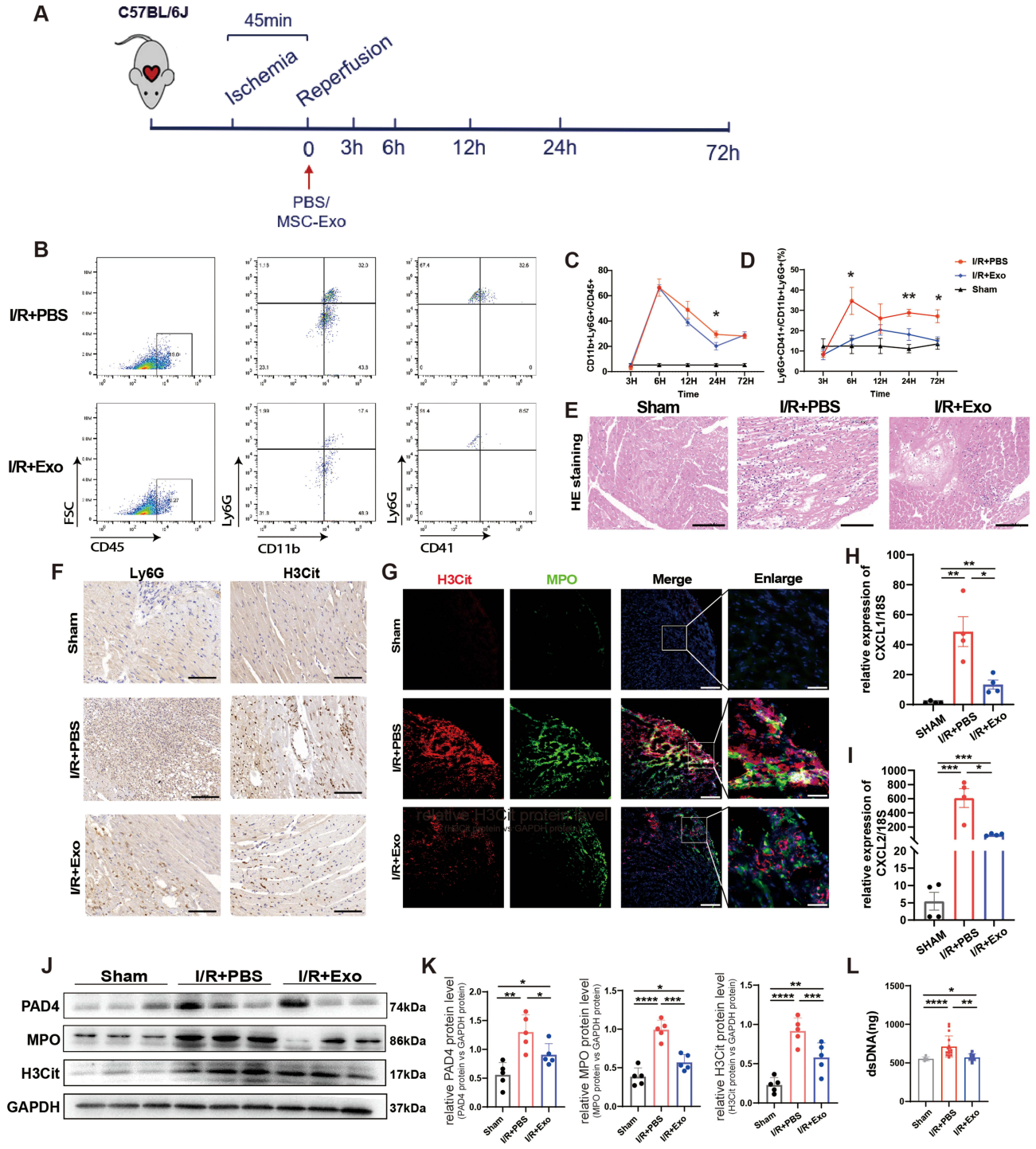

Figure 2 MSC-Exo reduced neutrophil infiltration and NETs release in vivo. (**A**) Schematic of the I/R model establishment, treatment, and tissue harvest for detection. (**B**–**D**) Representative flow cytometry scatter plot and statistical analysis of CD45+CD11b+Ly6G+neutrophils (**C**) and Ly6G+CD11b+CD41+ neutrophil-platelet complex (**D**) in the heart from mice treated with either MSC-Exo or PBS at 3, 6, 12, 24.72 hours after I/R or sham operation (n=5). (**E**) Representative images of HE staining in murine heart sections 24 hours after I/R injury in each group. Scale bar = 100 μm (n=4). (**F**) Representative immunohistochemical staining for Ly6G+ neutrophils and H3Cit+ NETs in heart sections 24 hours after I/R injury. Scale bar = 100 μm (n=5). (**G**) Representative immunofluorescence images for NETs formation staining with MPO (green), H3Cit (red) and DAPI (blue). Scale bar = 100 μm. Scale bar in Enlarge= 25 μm (n=5). (**H** and **I**) Relative gene expression of CXCL1 and CXCL2 in the hearts of mice sacrificed 24 hours after myocardial I/R injury (n=4). (**J** and **K**) Representative immune blots and the corresponding analysis of NETs pathways in the hearts of mice treated with PBS or MSC-Exo 24 hours after I/R (n=5). (**L**) Concentration of plasma dsDNA in Sham group (n=6), PBS-treated I/R group (n=12), MSC-Exo-treated I/R group (n=10). In panels (**C** and **D**), *P<0.05; **P<0.01 (two-way ANOVA followed by Bonferroni's multiple comparisons test). In panels (**H**, **I**, **K** and **L**), *P<0.05; **P<0.01; ***P<0.001; ****P < 0.0001 (one-way ANOVA with Bonferroni correction).

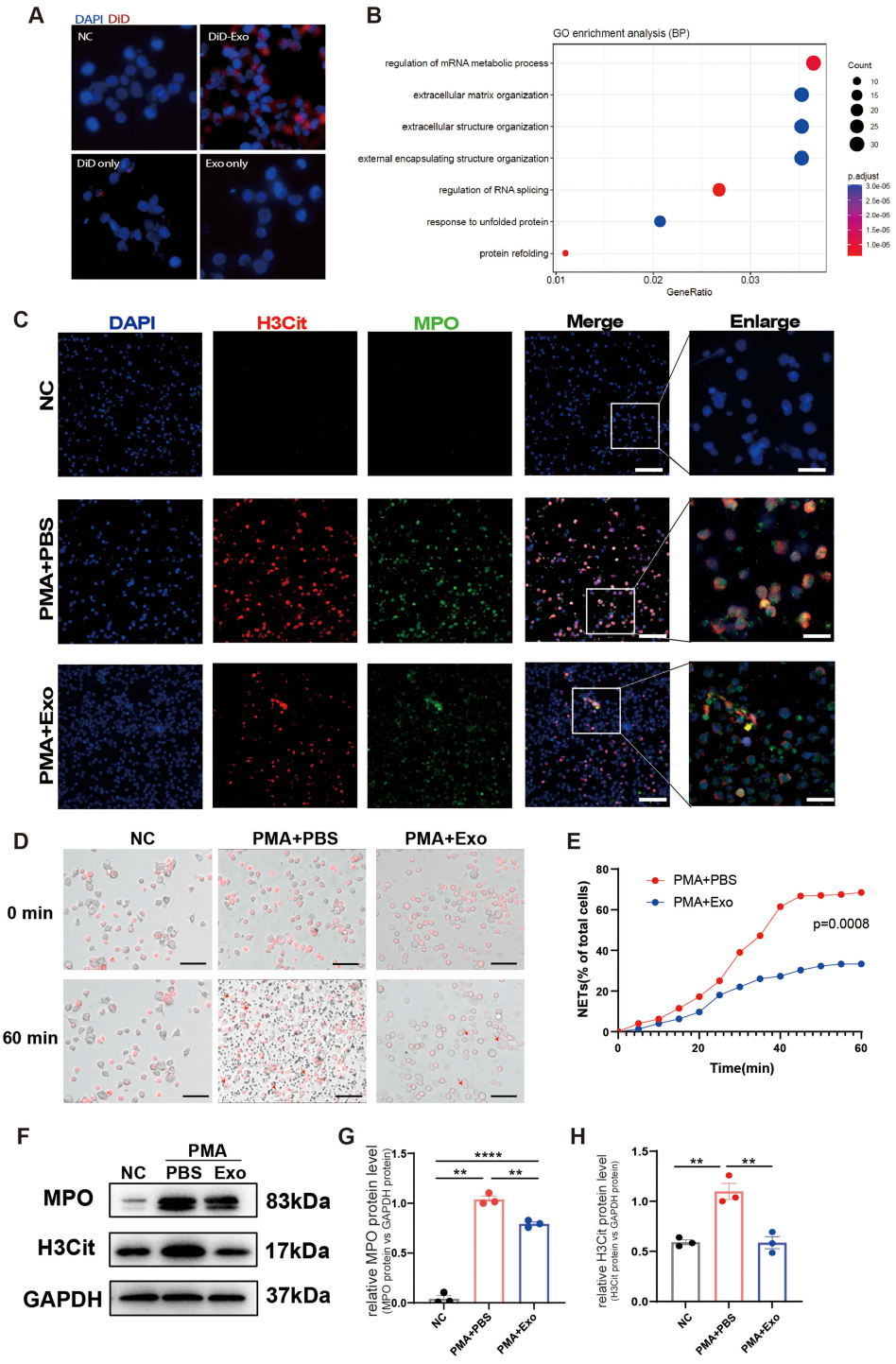

Figure 3 MSC-Exo reduced NETs formation in vitro. (**A**) Representative images of the uptake of DiD-labelled MSC-Exo (red) by primary neutrophils staining with DAPI (blue). DiD only group, PBS negative control stained DiD. Exo only group, background neutrophils fluorescence with non-stained MSC-Exo. Scale bar = 30 μm. (**B**) GO enrichment of the biological process category in primary neutrophils treated with PBS or MSC-Exo 12 hours after PMA stimulation. The top 7 down-regulated pathways after MSC-Exo treatment were presented and ranked. Sets were listed only if p <0.05. The extracellular matrix organization was found to be among the top down-regulated pathways in the MSC-Exo group (n=3 each group). (**C**) Representative immunofluorescence images for NETs formation staining with MPO (green), H3Cit (red) and DAPI (blue) in primary neutrophils treated with PBS or MSC-Exo 12 hours after PMA stimulation. Scale bar in Merge = 100μm.Scale bar in Enlarge= 30 μm. (**D** and **E**) Representative time-lapse differential interference contrast (DIC) spinning-disk confocal microscopy images (**D**) at indicated time intervals and arithmetic means (n=3) of the percentage of time course (**E**) of plasma membrane rupture (NETosis) in neutrophils treated with PBS or MSC-Exo after PMA stimulation. Red, DNA (siR-DNA); Red arrows indicate the area of plasma membrane rupture. Scale bar = 100 μm. (**F**–**H**) Representative immune blots and the corresponding analysis of NETs pathways in the hearts of mice treated with PBS or MSC-Exo 24 hours after I/R (n=3). In panel (**E**), p value as shown (two-way ANOVA followed by Bonferroni's multiple comparisons test). In panel (**G** and **H**), **P<0.01; ****P < 0.0001 (one-way ANOVA with Bonferroni correction).

After stimulated with PMA, the co-staining of H3Cit and MPO was significantly reduced in the MSC-Exo treatment group (Figure 3C). The live cell imaging experiments revealed that chromatin decondensation and DNA release into the cytosol happened and finally induced the NETosis in the first hour after adding PMA, while the MSC-Exo treatment inhibited the formation of NETosis (Figure 3D and E). Western blot analysis was consistent with those in vivo (Figure 3F–H). After being treated with MSC-Exo, the proportion of cells undergoing NETosis was significantly reduced. Our data have demonstrated that MSC-Exo inhibited neutrophils from releasing extracellular traps.

MSC-Exo Suppressed NLRP3 Signal Pathway and S100A8/A9 Release

NLR family pyrin domain containing 3 (NLRP3) inflammasome assembly is known as the classical inflammation pathway, which was proved to have effects on PAD4-dependent NETs formation.[24] We wondered whether the MSC-Exo influences NETosis via the NLRP3 pathway. As the data shows, the expression of NLRP3 inflammasome components (NLRP3, ASC, AIM, caspase1, IL-1β) was remarkably up-regulated in the I/R group and was suppressed by MSC-Exo treatment (Figure 4A–D and Figure S3A-E). Several studies have revealed that neutrophil releases alarmin proteins like S100A8/A9, which in turn prime the NLRP3 inflammasome.[11] Then the plasma concentration of S100A8/A9 dimer results indicated that significant suppression of secretion of S100A8/A9 by MSC-Exo treatment (Figure 4E–G). In vitro, experiments also showed the levels of NLRP3 inflammasome pathway were decreased in the MSC-Exo treated neutrophils (Figure 4H–K). In addition, MSC-Exo also inhibited the expression of S100A8/A9 dimer in the supernatant of PMA-stimulated primary neutrophils compared to the PBS-treated groups (Figure 4L–N). These data suggested that MSC-Exo might inhibit the activation of NLRP3 inflammasome by reducing the neutrophil secretion of S100A8/A9.

MSC-Exo Reduced MVO Formation and Preserved Cardiac Function After Myocardial I/R Injury

NETs have been proven a crucial driver in MVO formation, which is related to adverse ventricular remodeling.[19] Importantly, our clinical studies also demonstrated that the number of neutrophils and the formation of MVO are related to worse cardiac function (Figure 1G). The CMR images indicated MSC-Exo treatments reduced the formation of MVO (Figure 5A). Thioflavin S staining of murine cardiac tissues showed that MSC-Exo reduced the MVO formation during I/R injury (Figure 5B). Besides, the Dextran staining showed superior perfusion of injured myocardium in the MSC-Exo-treated group than that in the PBS-treated group (Figure 5C and D). Transthoracic echocardiography analysis revealed that murine cardiac function was improved by the MSC-Exo treatment in the I/R model (Figure 5E). The infarct size (IS/AAR) was reduced in the MSC-Exo group compared with the PBS-treated group (Figure 5H and I). Less proportion of apoptosis cells was observed in the myocardium after MSC treatment by TUNEL staining (Figure 5F and G). In addition, MSC-Exo significantly alleviated cardiac fibrosis in the long term (Figure 5J). Together, our results above indicated that MSC-Exo reduced MVO formation and preserve cardiac function after I/R injury.

Systemic Depletion of Neutrophils Reduced the Efficacy of MSC-Exo Therapy

Then we depleted the majority of neutrophils to verify whether the protective effect of MSC-Exo was neutrophil-dependent. After being given the Ly6g antibody, the counts of peripheral neutrophils dropped off by 70% within 48 hours (Figure S4A). Flow cytometry analysis revealed that the proportions of neutrophils in the heart had no significant difference among the MSC-Exo, Ly6G, or MSC-Exo+Ly6g group (Figure 6A and Figure S4B), as well as the ratio of binding to platelets (Figure 6B).

Echocardiography measurements showed that the improvement in EF% mediated by MSC-Exo was stronger than that mediated by Ly6g antibody in the early period of I/R injury. Importantly, even depletion of most neutrophils via Ly6g antibody, MSC-Exo still exhibited a protective effect on cardiac function (Figure 6C). This may be because MSC not only acts on neutrophils activation but also regulates macrophages functions as our previous report.[18] In addition, Evan's blue staining results showed that depletion of neutrophils reduced the infarcted area, but not as well as MSC-Exo treatment. As before, MSC-Exo also decreased the infarcted area while neutrophil depletion (Figure 6D–F). The MVO formation in the injured myocardium was reduced with insignificant differences among the three groups treated by MSC-

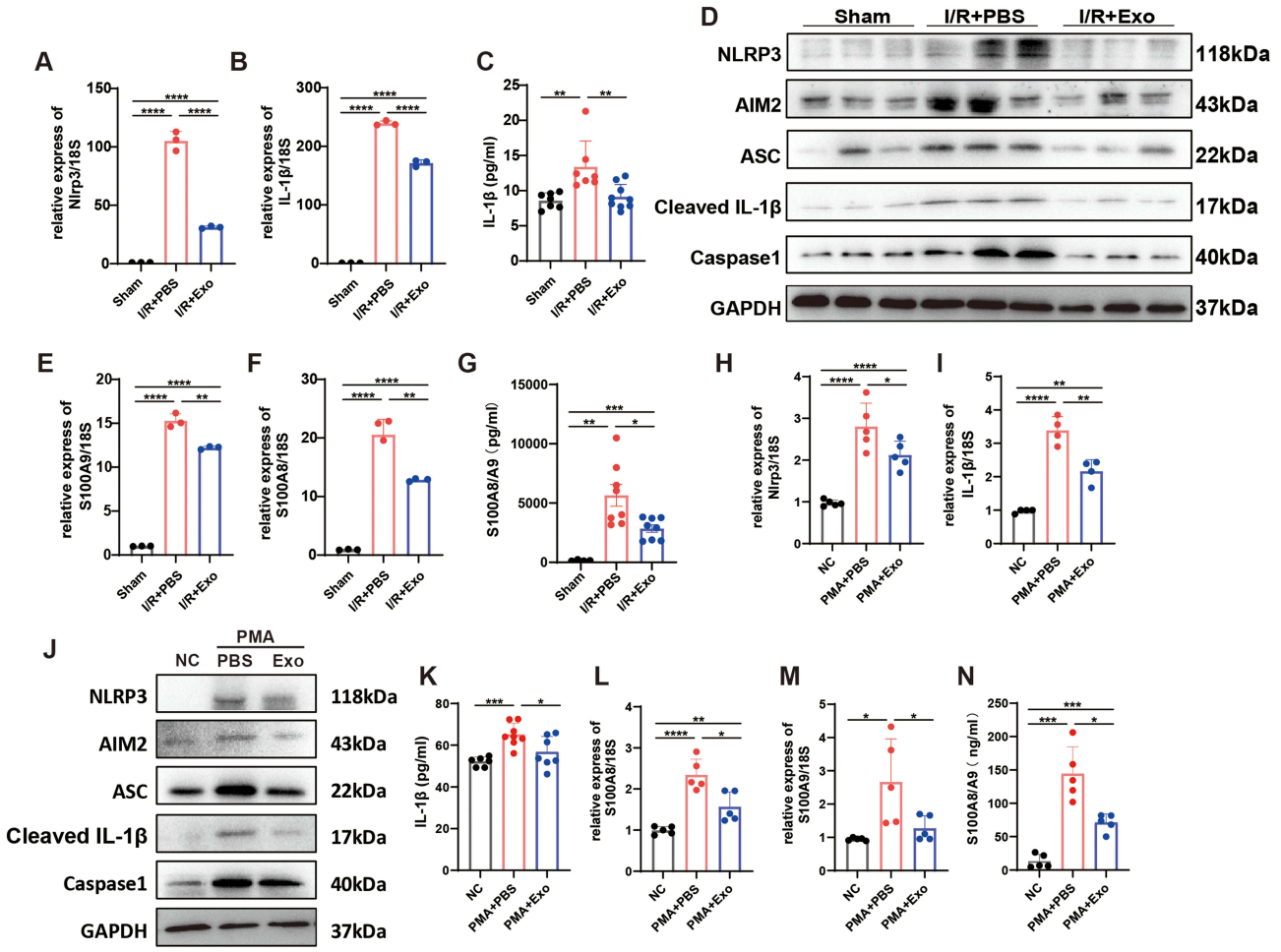

Figure 4 MSC-Exo suppressed NLRP3 signal pathway and S100A8/A9 release in vivo and in vitro. (**A** and **B**) Relative gene expression of NLRP3 and IL-1βin the hearts of mice sacrificed 24 hours after myocardial I/R injury (n=3). (**C**) Concentration of plasma IL-1β in Sham group (n=7), PBS-treated I/R group (n=7) and MSC-Exo-treated group (n=9). (**D**) Representative immune blots of the NLRP3 pathway in the hearts of mice treated with PBS or MSC-Exo 24 hours after I/R (n=3). (**E** and **F**) Relative gene expression of S100A9and S100A8in the hearts of mice sacrificed 24 hours after myocardial I/R injury (n=3). (**G**) Concentration of plasma S100A8/A9 in Sham group (n=5), PBS-treated I/R group (n=8) and MSC-Exo-treated group (n=8). (**H** and **I**) Relative gene expression of NLPR3and IL-1βin primary neutrophils treated with PBS or MSC-Exo 12 hours after PMA stimulation (n=5). (**J**) Representative immune blots of the NLRP3 pathway in primary neutrophils treated with PBS or MSC-Exo 24 hours after PMA stimulation (n=3). (**K**) Concentration of IL-1β in the supernatant of mouse neutrophils treated with PBS (n=8) or MSC-Exo (n=8) 24 hours after PMA stimulation or control (n=6). (**L** and **M**) Relative gene expression of S100A9and S100A8 in primary neutrophils treated with PBS or MSC-Exo 12 hours after PMA stimulation (n=5). (**N**) Concentration of S100A8/A9 in the supernatant of primary neutrophils treated with PBS or MSC-Exo 24 hours after PMA stimulation or control (n=5). In panels (**A–C**, **E–I**, **K–N**), *P<0.05; **P<0.01; ***P<0.001; ****P < 0.0001 (one-way ANOVA with Bonferroni correction).

Exo, anti-Ly6g, or both (Figure 6G–I). Moreover, HE staining and IHC results also showed no significant differences among the treated groups (Figure S4C–E). The above experiments show that the impact of MSC-Exo was partly dependent on its interactions with neutrophils.

MiR-199a Played a Part in MSC-Exo Mediated Therapeutic Effect

MSC-Exo was described as a miRNA carrier to affect the receptor cells. Our previous studies have sequenced the abundant miRNAs in the exosomes including mir-21, mir-22, mir-378, mir-182, and mir-199a.[18] Among these, we focused on mir-199, which was reported to suppress neutrophil migration and reduce inflammation.[25] To investigate whether mir-199 contributed to the MSC-Exo mediated decrease in NETs formation, we constructed mouse neutrophils with overexpression or knockdown of the mir-199a-3p or mir-199a-5p expression (Figure 7A). Compared with the negative control group after stimulation with PMA, the gene expression and protein expression of NETs-related pathways were significantly decreased in the mir-199a-3p or mir-199a-5p overexpression groups, and increased in the mir-199a-3p or mir-199a-5p knockout groups (Figure 7B and Figure S5).

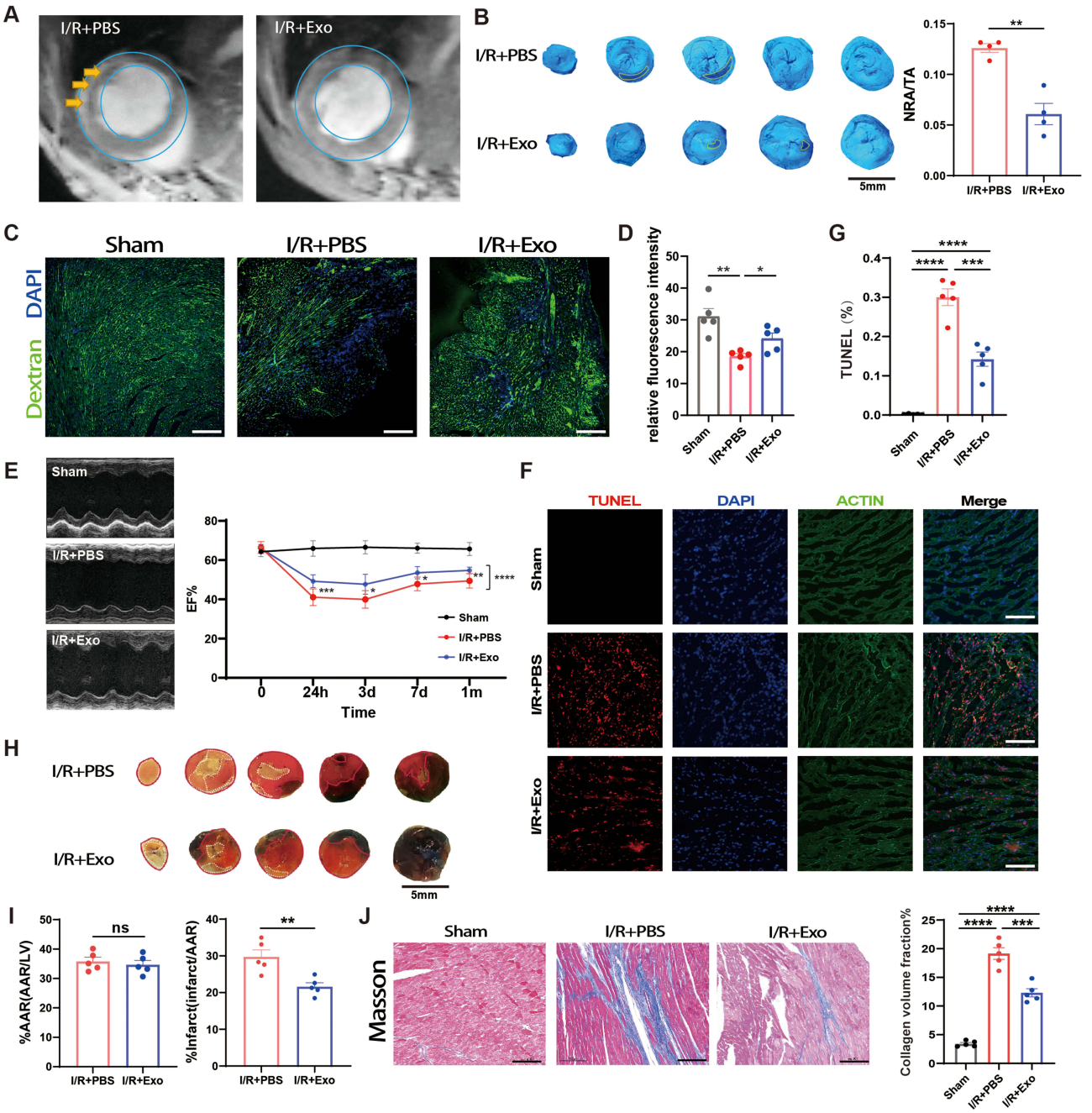

Figure 5 MSC-Exo reduced MVO formation and preserved cardiac function after myocardial I/R injury. (**A**) Representative end-diastolic static frames from LGE in midventricular short-axis in mice 7 days after I/R injury. Yellow arrowheads indicate MVO in the LV wall. (**B**) Representative thioflavin S staining under ultraviolet light in the hearts of mice sacrificed 3 days after myocardial I/R injury and the statistical comparisons of the ratio of the no-reflow area (NRA) to the total heart section area (TA) (n=5). (**C**) Representative FITC-dextran (green) angiographic micrographs in murine heart 3 days after I/R injury. (**D**) Quantification of fluorescence intensity in (**C**) (n=5). (**E**) Echocardiography measurements of cardiac functions of mice at 24 hours, 3 days, 7 days and 1 month after I/R or sham operation, LVEF values were measured (n=5). (**F**) Representative immunofluorescence images for TUNEL staining with TUNEL (red) and DAPI (blue). Scale bar = 100 μm. (**G**) Quantitative analysis of TUNEL-positive nuclei. (**H**) Images illustrate representative sections of Evan's blue and TTC double-stained hearts from mice treated with PBS or MSC-Exo 3 days after I/R. (**I**) Quantitative analysis of the percentage AAR and percentage infarct of hearts (n=5 each group). (**J**) Representative images and quantitative analysis of Masson staining in heart sections 1 month post-I/R (n=5 each group). In panels B and I, **P<0.01; ns, not significant (unpaired two-tailed Student's *t*-test). In panels (**D** and **G**), *P<0.05; **P<0.01; ***P < 0.001; ****P < 0.0001 (one-way ANOVA with Bonferroni correction). In panel (**E**), *P<0.05; **P<0.01; ***P < 0.001; ****P < 0.0001 (two-way ANOVA followed by Bonferroni's multiple comparisons test).

To confirm that MSC-Exo affects neutrophils through mir-199a, we constructed MSCs with knocked-down mir-199a-5p or mir-199a-3p, collected exosomes in the same way. The decrease of mir-199a-5p or mir-199a-3p expression within the exosomes was verified (Figure 7C). Immunofluorescence showed that after PMA stimulation, there was little difference between neutrophils treated with mir-199a-5p or mir-199a-3p inhibitor MSC-Exo and those treated with

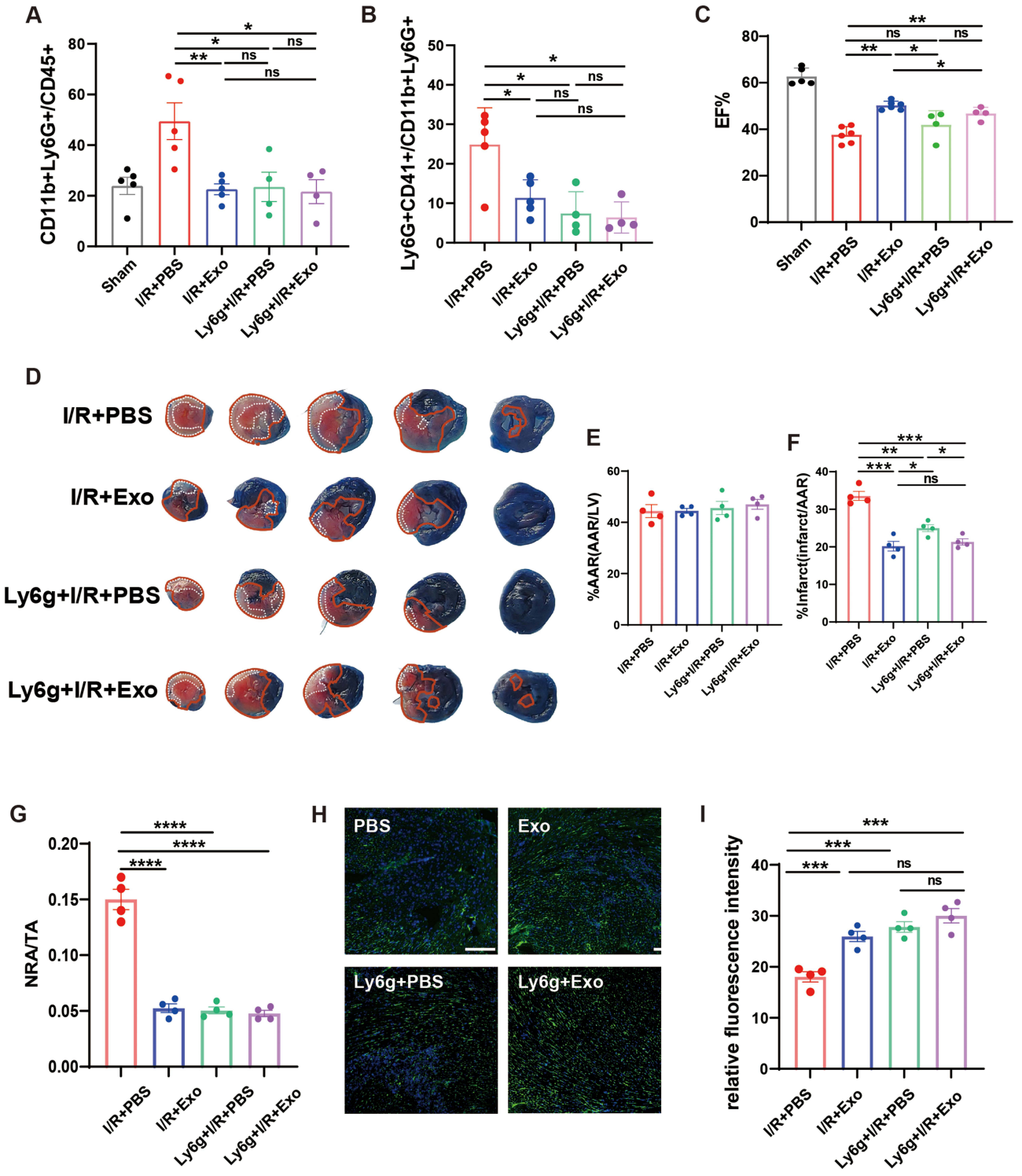

Figure 6 Systemic depletion of neutrophils reduced the efficacy of MSC-Exo treatment after I/R injury. (**A** and **B**) Flow cytometry statistical analysis of CD45+CD11b+Ly6G + neutrophils (**A**) and Ly6G+CD11b+CD41+ neutrophil-platelet complex (**B**) in the heart from mice sacrificed 3 days after injection of either MSC-Exo or PBS with (n=4) or without (n=5) neutrophil depletion prior to myocardial I/R injury or in Sham group (n=4). (**C**) Echocardiography measurements of cardiac functions of mice at 3 days after I/R (n=4). (**D**) Images illustrate representative sections of Evan's blue and TTC double-stained hearts from mice 3 days after I/R. (**E** and **F**) Quantitative analysis of the ratio of AAR (**E**)and infarct area of hearts (**F**) (n=4). (**G**) Statistical comparisons of the ratio of the no-reflow area (NR) to the total heart section area (TA) by thioflavin S staining (n=4). (**H**) Representative FITC-dextran (green) angiographic micrographs in murine heart 3 days after I/R injury. (**I**) Quantification of fluorescence intensity in (**H**) (n=4). In panels (**A**–**C**, **E**–**G** and **I**), *P<0.05; **P<0.01; ***P<0.001; ****P < 0.0001; ns, not significant (one-way ANOVA with Bonferroni correction).

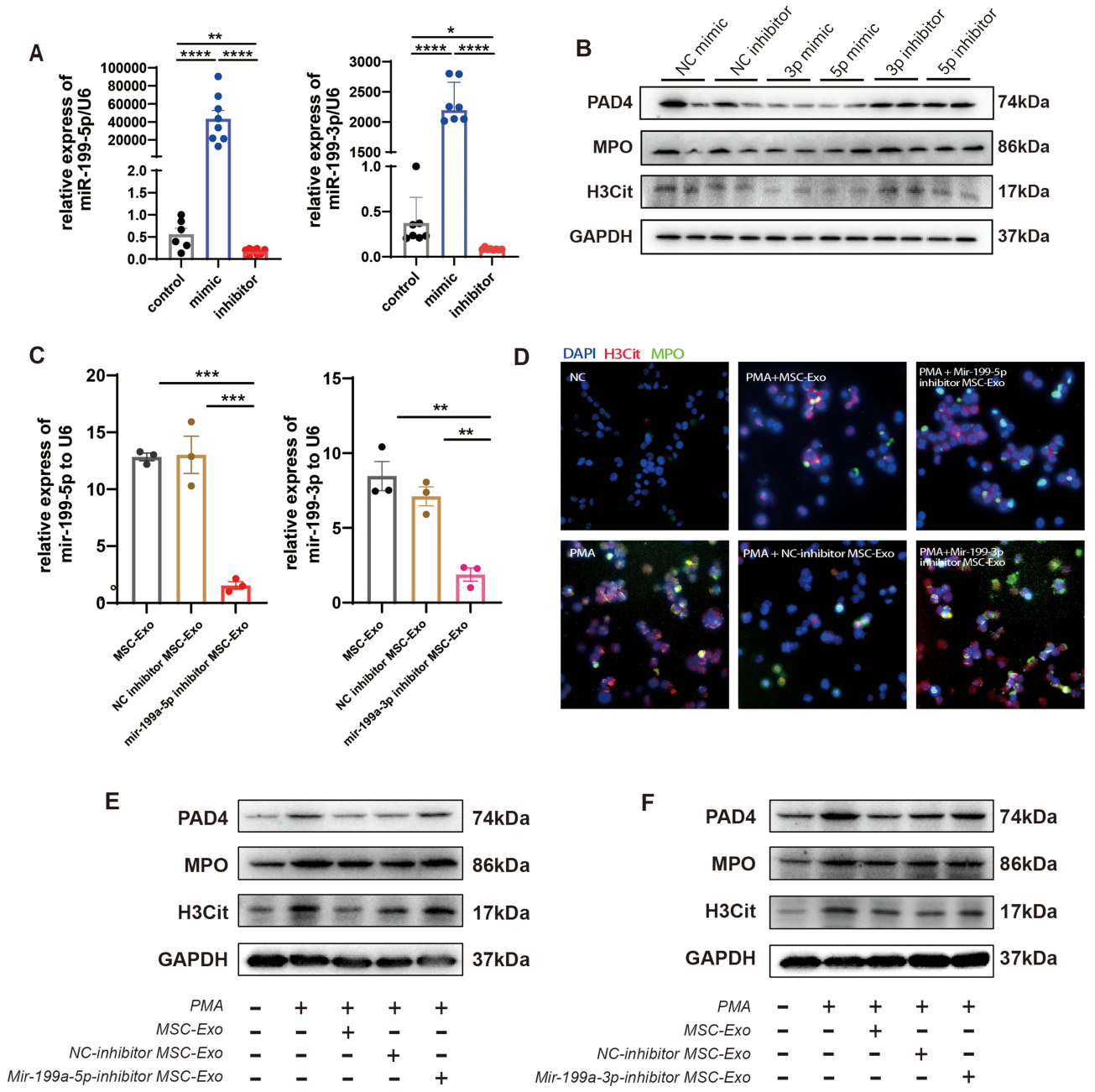

Figure 7 Mir-199a contributed to the therapeutic effect mediated by MSC-Exo. (**A**) Relative gene expression of miR-199-5p and mir-199-3p levels in neutrophils treated with mimic or inhibitor (n=7). The expression levels of the miRNAs were normalized to U6. (**B**) Representative immune blots of PAD4, MPO and H3Cit in neutrophils after 24 hours of PMA stimulation following mimic or inhibitor treatment (n=3). (**C**) Relative gene expression of miR-199-5p and mir-199-3p levels in MSC-Exo isolated from MSCs treated with inhibitor (n=3). The expression levels of the miRNAs were normalized to U6. (**D**) Representative immunofluorescence images for NETs formation staining with MPO (green), H3Cit (red) and DAPI (blue) in primary neutrophils with MSC-Exo, NC-inhibitor MSC-Exo, mir-199a-5p inhibitor MSC-Exo or mir-199a-3p MSC-Exo treatment 12 hours after PMA stimulation. Scale bar in Merge = 50μm (n=3). (**E** and **F**) Representative immune blots of PAD4, MPO and H3Cit in neutrophils after 24 hours of PMA stimulation following MSC-Exo, NC-inhibitor MSC-Exo, mir-199a-5p inhibitor MSC-Exo or mir-199a-3p MSC-Exo inhibitor treatment (n=3). In panels (**A** and **C**), *P<0.05; **P<0.01; ***P<0.001; ****P < 0.0001 (one-way ANOVA with Bonferroni correction).

PBS in terms of NETs release (Figure 7D). Western Blot results showed an increase in NETs related expression (Figure 7E and F, Figure S6) in mir-199a-5p or mir-199a-3p inhibitor MSC-Exo group, compared with the MSC-Exo group. These results further confirmed our hypothesis.

These results indicated that mir-199a may be an important downstream factor of MSC-Exo in the suppression of neutrophil activation.

Discussion

Collectively in this study, we demonstrated that MSC-Exo treatment remarkably prohibited the infiltration of neutrophils in to the injured myocardium and attenuated the inflammatory response in a murine model of myocardial I/R injury. MSC-Exo treatment exerted cardioprotective effects by attenuating myocardial MVO formation and preserving cardiac function through its anti-inflammatory properties. Furthermore, we observed that MSC-Exo reduced the NETs formation of neutrophils and suppressed NLRP3 inflammasome activation. The secretion of S100A8/A9 was also decreased after MSC-Exo treatment. Neutrophil depletion model revealed that neutrophils were mainly the downstream target of MSC-Exo. Notably, we identified mir-199 as a key component in MSC-Exo responsible for inhibiting neutrophil function.

Currently, the regulation of inflammation response following I/R injury is a hot and difficult topic in cardiovascular research. In recent years, several strategies targeting pro-inflammatory M1 macrophages to mitigate inflammation levels or regulating the transition of macrophages from a pro-inflammatory M1 phenotype to an anti-inflammatory M2 phenotype to promote repair.[18,26,27] However, neutrophils play a primary role in initiating the inflammatory storm, instead of macrophages.[28] Furthermore, the inhibition of monocyte-macrophages will impede the subsequent repair process.[29] Our results showed that the number of neutrophils exhibited a significant increase at 3 hours post-reperfusion, peaking between 6–48 hours (in Figure 2), preceding the recruitment of other inflammatory cells. Neutrophils are also the largest number of immune cells and act as a driver in the inflammation storm. Both previous studies[8,19] and our experimental findings have demonstrated a strong correlation in AMI patients between the number of neutrophils and MVO, which significantly impacts left ventricular function and clinical prognosis (in Figure 1). In addition to releasing a plethora of inflammatory factors, activated neutrophils can also promote the formation of NETs, which serve as a scaffold for thrombus formation and contribute to MVO development. This reaction effectively curtails bacterial inflammation by limiting its spread.[24] However, the formation of MVO during I/R injury can lead to poor perfusion in the infarct area and exacerbate myocardial injury. The number of neutrophils, the formation of NETs, and the secretion of S100A8/A9 of neutrophils were significantly different in patients with and without MVO (in Figure 1), which is in line with the findings of other relevant literature. The purpose of this project is to develop a more effective strategy for regulating the inflammatory storm caused by neutrophils, which are the most rapidly recruited and abundant inflammatory cells during the acute phase. We have previously reported that intramyocardial injection of MSC-Exo exerts a potent immunomodulatory effect in the context of cardiovascular disease.[18] In this study, we aimed to achieve clinical transformation by utilizing intravenous injection of MSC-Exo to target neutrophils and suppress inflammation response in I/R while preserving the repair process. Our results demonstrated that MSC-Exo inhibited the mobilization of neutrophils by reducing the secretion of chemokines such as CXLCL1 and CXCL2 (in Figure 2), [which resulted in the decrease of neutrophil infiltration in blood and then in damaged myocardium]. The flow cytometry and histochemistry analyses revealed a decrease in neutrophil infiltration in the myocardium with MSC-Exo injection. Finally, magnetic resonance imaging and echocardiography showed a reduction in MVO formation and preservation of cardiac function after MSC-Exo treatments (in Figure 4). These results suggested that MSC-Exo exhibited a potent inhibitory effect on neutrophil activation following I/R injury. Besides, the recruitment of neutrophils is a prerequisite for the activation of macrophages. The inhibition of neutrophil infiltration and function leads to a decrease in pro-inflammatory macrophage numbers after I/R.[30] Our research further demonstrates the comprehensive and potent immunomodulatory effects of MSC-Exo.

The sequencing results in Figure 2 showed that MSC-Exo may modulate the neutrophil expression in terms of extracellular matrix composition and nuclear or cell membrane functions. In the process of NETs formation, the release of DNA from the nucleus to extracellular space necessitates nuclear membrane rupture, and extensive cytoskeletal and organelle remodeling. Then we speculated that MSC-Exo may affect the formation of NETs in neutrophils. The flow cytometry data indicated the absence of differences in NETs in blood samples, which was attributed to their rarity (in Figure S2). Notably, a significant reduction of NETs was observed after treatment with MSC-Exo in the heart. The results obtained from CMR and thioflavin S staining demonstrated a decrease in MVO by MSC-Exo treatment. After the depletion of neutrophils, the beneficial effect of MSC-Exo on MVO was attenuated (in Figure 6). These results confirmed that MSC-Exo inhibited the formation of MVO following I/R

by targeting neutrophils. However, even in the absence of neutrophils, MSC-Exo still demonstrated a certain degree of improvement in cardiac function, which may be partially attributed to their ability to modulate macrophages.

S100A8/A9 is a sensitive chemotactic reactant specifically secreted by neutrophils as an alarm signal. The release of S100A8/A9 within the myocardium promotes further leukocyte recruitment and augments pro-inflammatory cytokine secretion. Recently, Goran M et al reported that the short-term administration of S100A9-specific inhibitors can effectively inhibit the infiltration of immune cells into tissues after infarction.[31] However, prolonged use may impede subsequent repair processes and compromise protective effects.[32] The above evidence also confirms that the inflammatory process is a complex and continuous pathological process that should not be blindly blocked. Instead, neutrophil activation should be moderately suppressed during the peak of inflammation in the early stage of I/R injury to regulate inflammation without compromising myocardial repair. Based on the above consensus, the application of MSC-Exo in our research is limited to early and short-term use due to its short life cycle. Blood transfusion of MSC-Exo can accumulate in injured tissues but is rapidly cleared within 24 hours by the liver and spleen.[33] As a result, neutrophils would be suppressed by MSC-Exo only at the acute pro-inflammatory phase in the initial time of I/R, which did not affect the subsequent repairment. In addition, the long-term pathological results demonstrated that the ventricular remodeling and fibrosis following I/R injury were both attenuated by MSC-Exo treatment, which showed a standing beneficial effect of MSC-Exo on the initial phase of myocardial I/R (in Figure 5).

Some studies have reported that the secretion of S100A8/A9 promotes the activation of NLRP3[11] and NLRP3 inflammasome promotes the formation of NETs.[34] These processes create a vicious loop that amplifies the inflammatory response. Our research revealed MSC-Exo is involved in the regulation of NLRP3 inflammasome (in Figure 4). Our findings demonstrated that the levels of NLRP3 inflammasome and pro-inflammatory cytokine IL-1β in the neutrophils were up-regulated following I/R, and MSC-Exo treatment abrogated the activation of NLRP3 inflammasome in neutrophils, suggesting that NLRP3 might be the downstream target of MSC-Exo in suppressing the NETs formation. MSC-Exo effectively disrupts the vicious cycle of S100A8/A9-NLRP3-NETs and exerts a potent overall inhibitory effect on neutrophils.

The abundant miRNA expression within MSC-Exo plays a crucial role in its immune regulation. As shown in the previous study, mir-199a expression exhibited a peak height in the MSC-Exo,[18] which has been previously reported to inhibit neutrophil chemotaxis.[25] We conducted experiments using mir-199a mimics and observed that they were capable of achieving a protective effect equivalent to that of MSC-Exo (in Figure 7). Furthermore, we employed siRNA to interfere with the expression of mir-199a, and our findings indicated that the protective effect was abolished. The downregulation of mir-199a in MSC-Exo also attenuated its ability to reduce NETs formation. These results suggest that mir-199a is a key factor for MSC-Exo in inhibiting neutrophils, particularly in improving the inflammatory response during the acute phase of I/R injury.

The limitation of this study is the application of MSC-Exo was observed only during the acute phase, further research is necessary to determine whether multiple administrations of MSC-Exo may yield superior out comes in the long-term. Besides, the anti-inflammatory efficacy of mir-199 has not been verified in vivo, and the transformation value of mir-199 needs to be further studied in the future.

Conclusion

Our study demonstrates that MSC-derived exosomes attenuate myocardial I/R injury by reducing neutrophil infiltration and NETs formation within the heart. Mir-199 packaged in MSC-Exo is involved in the modulation of neutrophil function by targeting NLRP3 inflammasome activation. Our study provides a theoretical foundation for a protective effect of MSC-Exo and furnishes novel evidence supporting the clinical translation.

Funding

This work was supported by the Natural Science Foundation of China (grant numbers 8207081148 and 82100525), China Postdoctoral Science Foundation (grant number 2021T140316), Jiangsu Natural Science Foundation (grant number BK20210013) and the Funds for Distinguished Young Scientists in Nanjing (JQX22001).

Disclosure

The authors report no conflicts of interest in this work.

References

1. Heusch G. Myocardial ischaemia-reperfusion injury and cardioprotection in perspective. *Nat Rev Cardiol*. 2020;17(12):773–789. doi:10.1038/s41569-020-0403-y
2. Algoet M, Janssens S, Himmelreich U, et al. Myocardial ischemia-reperfusion injury and the influence of inflammation. *Trends Cardiovasc Med*. 2022;33:357–366. doi:10.1016/j.tcm.2022.02.005
3. Zhang RYK, Cochran BJ, Thomas SR, Rye KA. Impact of reperfusion on temporal immune cell dynamics after myocardial infarction. *J Am Heart Assoc*. 2023;12:4.
4. Piccolo EB, Thorp EB, Sumagin R. Functional implications of neutrophil metabolism during ischemic tissue repair. *Curr Opin Pharmacol*. 2022;63:102191. doi:10.1016/j.coph.2022.102191
5. Sreejit G, Johnson J, Jaggers RM, et al. Neutrophils in cardiovascular disease, warmongers, peacemakers, or both? *Cardiovasc Res*. 2022;118(12):2596–2609. doi:10.1093/cvr/cvab302
6. Thiam HR, Wong SL, Wagner DD, Waterman CM. Cellular mechanisms of NETosis. *Annu Rev Cell Dev Biol*. 2020;36:191–218. doi:10.1146/annurev-cellbio-020520-111016
7. Perdomo J, Leung HHL, Ahmadi Z, et al. Neutrophil activation and NETosis are the major drivers of thrombosis in heparin-induced thrombocytopenia. *Nat Commun*. 2019;10(1):1322. doi:10.1038/s41467-019-09160-7
8. Ge L, Zhou X, Ji WJ, et al. Neutrophil extracellular traps in ischemia-reperfusion injury-induced myocardial no-reflow, therapeutic potential of DNase-based reperfusion strategy. *Am J Physiol Heart Circ Physiol*. 2015;308(5):H500–9. doi:10.1152/ajpheart.00381.2014
9. Fresneda Alarcon M, McLaren Z, Wright HL. Neutrophils in the pathogenesis of rheumatoid arthritis and systemic lupus erythematosus, same foe different M.O. *Front Immunol*. 2021;12:649693. doi:10.3389/fimmu.2021.649693
10. Papayannopoulos V, Metzler KD, Hakkim A, Zychlinsky A. Neutrophil elastase and myeloperoxidase regulate the formation of neutrophil extracellular traps. *J Cell Biol*. 2010;191(3):677–691. doi:10.1083/jcb.201006052
11. Sreejit G, Abdel-Latif A, Athmanathan B, et al. Neutrophil-Derived S100A8/A9 amplify granulopoiesis after myocardial infarction. *Circulation*. 2020;141(13):1080–1094. doi:10.1161/CIRCULATIONAHA.119.043833
12. Wang S, Song R, Wang Z, Jing Z, Wang S, Ma J. S100A8/A9 in Inflammation. *Front Immunol*. 2018;9:1298. doi:10.3389/fimmu.2018.01298
13. Chen TJ, Yeh YT, Peng FS, Li AH, Wu SC. S100A8/A9 enhances immunomodulatory and tissue-repairing properties of human amniotic mesenchymal stem cells in myocardial ischemia-reperfusion injury. *Int J Mol Sci*. 2021;22:20.
14. Shi Y, Wang Y, Li Q, et al. Immunoregulatory mechanisms of mesenchymal stem and stromal cells in inflammatory diseases. *Nat Rev Nephrol*. 2018;14(8):493–507. doi:10.1038/s41581-018-0023-5
15. Hoang DM, Pham PT, Bach TQ, et al. Stem cell-based therapy for human diseases. *Signal Transduct Target Ther*. 2022;7(1):272. doi:10.1038/s41392-022-01134-4
16. Coppin L, Sokal E, Stephenne X. Thrombogenic risk induced by intravascular mesenchymal stem cell therapy, current status and future perspectives. *Cells*. 2019;8(10):1160. doi:10.3390/cells8101160
17. Harrell CR, Jovicic N, Djonov V, Arsenijevic N, Volarevic V. Mesenchymal stem cell-derived exosomes and other extracellular vesicles as new remedies in the therapy of inflammatory diseases. *Cells*. 2019;8(12):1605. doi:10.3390/cells8121605
18. Zhao J, Li X, Hu J, et al. Mesenchymal stromal cell-derived exosomes attenuate myocardial ischaemia-reperfusion injury through miR-182-regulated macrophage polarization. *Cardiovasc Res*. 2019;115(7):1205–1216. doi:10.1093/cvr/cvz040
19. Garcia-Prieto J, Villena-Gutierrez R, Gomez M, et al. Neutrophil stunning by metoprolol reduces infarct size. *Nat Commun*. 2017;8:14780. doi:10.1038/ncomms14780
20. Qiao S, Zhang W, Yin Y, et al. Extracellular vesicles derived from Kruppel-Like Factor 2-overexpressing endothelial cells attenuate myocardial ischemia-reperfusion injury by preventing Ly6C(high) monocyte recruitment. *Theranostics*. 2020;10(25):11562–11579. doi:10.7150/thno.45459
21. An Z, Tian J, Liu Y, et al. Exosomes as a cell-free therapy for myocardial injury following acute myocardial infarction or ischemic reperfusion. *Aging Dis*. 2022;13:1770–1786. doi:10.14336/AD.2022.0416
22. Arslan F, Lai RC, Smeets MB, et al. Mesenchymal stem cell-derived exosomes increase ATP levels, decrease oxidative stress and activate PI3K/Akt pathway to enhance myocardial viability and prevent adverse remodeling after myocardial ischemia/reperfusion injury. *Stem Cell Res*. 2013;10:301–312. doi:10.1016/j.scr.2013.01.002
23. Dou H, Kotini A, Liu W, et al. Oxidized phospholipids promote NETosis and Arterial Thrombosis in LNK(SH2B3) deficiency. *Circulation*. 2021;144:1940–1954. doi:10.1161/CIRCULATIONAHA.121.056414
24. Thiam HR, Wong SL, Qiu R, et al. NETosis proceeds by cytoskeleton and endomembrane disassembly and PAD4-mediated chromatin decondensation and nuclear envelope rupture. *Proc Natl Acad Sci U S A*. 2020;117(13):7326–7337. doi:10.1073/pnas.1909546117
25. Hsu AY, Wang D, Liu S, et al. Phenotypical microRNA screen reveals a noncanonical role of CDK2 in regulating neutrophil migration. *Proc Natl Acad Sci U S A*. 2019;116(37):18561–18570. doi:10.1073/pnas.1905221116
26. Lu S, Tian Y, Luo Y, et al. Iminostilbene, a novel small-molecule modulator of PKM2, suppresses macrophage inflammation in myocardial ischemia-reperfusion injury. *J Adv Res*. 2021;29:83–94. doi:10.1016/j.jare.2020.09.001

27. Dong X, Jiang J, Lin Z, et al. Nuanxinkang protects against ischemia/reperfusion-induced heart failure through regulating IKKbeta/IkappaBalpha/NF-kappaB-mediated macrophage polarization. *Phytomedicine*. 2022;101:154093. doi:10.1016/j.phymed.2022.154093
28. Yan X, Anzai A, Katsumata Y, et al. Temporal dynamics of cardiac immune cell accumulation following acute myocardial infarction. *J Mol Cell Cardiol*. 2013;62:24–35. doi:10.1016/j.yjmcc.2013.04.023
29. de Couto G, Liu W, Tseliou E, et al. Macrophages mediate cardioprotective cellular postconditioning in acute myocardial infarction. *J Clin Invest*. 2015;125(8):3147–3162. doi:10.1172/JCI81321
30. Selders GS, Fetz AE, Radic MZ, Bowlin GL. An overview of the role of neutrophils in innate immunity, inflammation and host-biomaterial integration. *Regen Biomater*. 2017;4(1):55–68. doi:10.1093/rb/rbw041
31. Marinkovic G, Grauen Larsen H, Yndigegn T, et al. Inhibition of pro-inflammatory myeloid cell responses by short-term S100A9 blockade improves cardiac function after myocardial infarction. *Eur Heart J*. 2019;40(32):2713–2723. doi:10.1093/eurheartj/ehz461
32. Marinkovic G, Koenis DS, de Camp L, et al. S100A9 links inflammation and repair in myocardial infarction. *Circ Res*. 2020;127(5):664–676. doi:10.1161/CIRCRESAHA.120.315865
33. Krainska MM, Pietrzkowska N, Turlej E, Zongjin L, Marycz K. Extracellular vesicles derived from mesenchymal stem cells as a potential therapeutic agent in acute kidney injury (AKI) in felines, review and perspectives. *Stem Cell Res Ther*. 2021;12(1):504. doi:10.1186/s13287-021-02573-6
34. Munzer P, Negro R, Fukui S, et al. NLRP3 inflammasome assembly in neutrophils is supported by PAD4 and Promotes NETosis under sterile conditions. *Front Immunol*. 2021;12:683803. doi:10.3389/fimmu.2021.683803